

Enhanced co-solubilities of Ca and Si in YAG ($\text{Y}_3\text{Al}_5\text{O}_{12}$)

Yener Kuru*, Erdem Onur Savasir, Saide Zeynep Nergiz, Cinar Oncel, and Mehmet Ali Gulgun

Sabancı University, FENS, Orhanli-Tuzla, 34956 Istanbul, Turkey

Received 1 July 2007, accepted 18 March 2008

Published online 19 June 2008

PACS 64.75.-g, 81.05.Je

* Corresponding author: e-mail yenerk@su.sabanciuniv.edu, Phone: +49 711 689 1377, Fax: +49 711 689 1389

General garnet structure (Ia3d) is a forgiving host and can accommodate cations of varying sizes and valence states. Studies on highly yttrium doped alumina ceramics with Ca and Si contamination indicated that YAG precipitates in the ceramic had a propensity to allow simultaneous incorporation of small amounts of Ca and Si impurities in their structure. In this study, using chemical synthesis techniques it was shown that YAG can accommodate up to approximately 8 cation % Ca^{+2} and Si^{+4} (i.e. $\text{Ca}^{+2}/\text{Y}^{+3}$ and $\text{Si}^{+4}/\text{Y}^{+3}$) if they are incorporated together. Equilibrium conditions are established by calcining sam-

ples at 900 °C for 2 hours and cooling the samples to room temperature in the furnace. Disappearing-phase method and energy dispersive X-ray spectroscopy were used to determine solubility and co-solubility limits. Beyond the solubility limit phase separation occurred and three crystalline yttrium aluminate phases (YAG, YAP (yttrium aluminate perovskite, YAlO_3), YAM (yttrium aluminate monoclinic, $\text{Y}_4\text{Al}_2\text{O}_9$)) were observed. It is believed that the excess Ca and Si above co-solubility limit precipitate out in the form of an x-ray amorphous anorthite-like glass in the system.

© 2008 WILEY-VCH Verlag GmbH & Co. KGaA, Weinheim

1 Introduction Yttrium aluminum garnet, $\text{Y}_3\text{Al}_5\text{O}_{12}$ (YAG), drew considerable attention as a host for solid-state industrial, medical and scientific laser applications. YAG is known to be a very forgiving host material and can be heavily doped with cations of different sizes and valence states. In addition to this YAG is one of the best high temperature structural oxides known [1]. The lasing substances such as neodymium, erbium, ytterbium, chromium, thulium, or holmium can be incorporated into the matrix of YAG in suitable concentrations. Nd:YAG is one of the best laser materials for the high power, high energy and Q-switched pulse laser systems and it is used for distance measuring, chemical large-distance analysis, laser drilling, pointer for electronic vision etc. Compared to the commonly used Nd:YAG crystal, another doped crystal Yb:YAG has a larger absorption bandwidth and it is known as a good laser gain material. In the case of Yb:YAG doping level as high as 50 at.% has been reported [2]. Yet another laser crystal, Er:YAG produces “eye-safe” wavelengths for many applications where human eyes could be injured. Their excellent optical, high temperature mechanical properties and chemical stability, suggest YAG ceramics as the most promising materials for solid-state laser application. Moreover, some of its high temperature mechanical proper-

ties open YAG new application fields like fiber reinforcements in ceramic and metal-matrix composite materials that withstand very high temperatures as advanced structural materials [3].

One way of substituting cations is introduction of a cation similar in size and charge to one of the original cations, other ways include the substitution of two cations that have similar size but different charges, one greater and the other less than those of the original cations [4]. It was shown by Yoder and Keith that there is a complete solid solution series between garnet mineral spessartite ($\text{Mn}_3\text{Al}_2(\text{SiO}_4)_3$) and yttrium aluminate garnet (YAG, $\text{Y}_3\text{Al}_5\text{O}_{12}$). Yttrium can be substituted for manganese if aluminum is simultaneously substituted for silicon to maintain charge balance in the structure [5]. Carda pointed out that garnet solid solutions can be synthesized between $\text{Y}_3\text{Al}_2\text{Al}_3\text{O}_{12}$ (YAG) and $\text{Ca}_3\text{Cr}_2\text{Si}_3\text{O}_{12}$ [6].

Ca and Si are known to have very low solubilities in YAG. It was reported that Ca concentrations of 300-400 ppm cause precipitation of the second phase, which is an indication of the exceeded solubility limit [7,8]. However, Rotman and co-workers stated that solubility of Ca in YAG is approximately 840 ppm [9,10]; this is greater than the limit reported by Schuh. It should be here noted that the

samples employed by Rotman *et al.* had some Ce co-dopants. Solubility of Si was investigated by Sun *et al.* [11]; it was suspicious whether some small amount of Si was present in YAG or not. Detection limit of EDS is probably not sufficient to probe the solubility limit of Si. Vrolijk found out that solubility limit is larger than 600 ppm [7]. In addition, Wang *et al.* have recently reported that addition of 0.1 % Si to YAG leads to formation of secondary and tertiary phases (YAP and an amorphous phase, respectively), which is in agreement with the results of Sun [11,12]. Consequently, solubility limit of Si should be in the range between 600 ppm and 0.1 %.

In this paper, we report that YAG can be contaminated by large amounts of Ca and Si when they are simultaneously incorporated in contrast to their low elemental solubilities in YAG. Fig. 1 shows crystal structure of YAG and possible positions of Ca and Si impurities in the lattice. Conservation of charge balance in the structure during the substitution and solid solution between $Y_3Al_2Al_3O_{12}$ (YAG) and $Ca_3Al_2Si_3O_{12}$ (grossular) is thought to be responsible for this increased co-solubility limit.

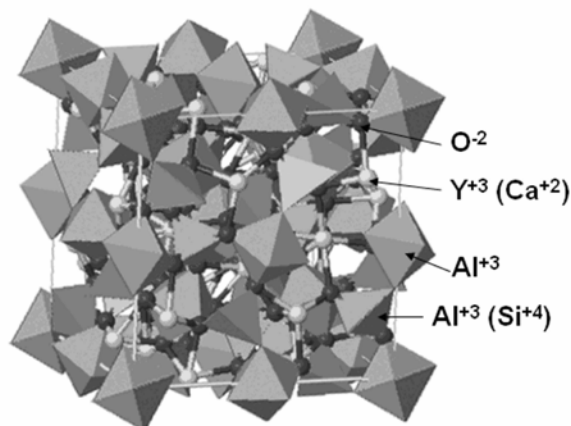


Figure 1 Crystal structure of YAG.

2 Experimental Aluminum nitrate nanohydrate ($Al(NO_3)_3 \cdot 9H_2O$, purity > 98 %, Fluka Chemie, Buchs, Switzerland), calcium nitrate tetrahydrate ($Ca(NO_3)_2 \cdot 4H_2O$, purity > 99 %, Merck KGaA, Darmstadt, Germany), yttrium nitrate hexahydrate ($Y(NO_3)_3 \cdot 6H_2O$, purity > 99.9 %, Aldrich Chemical Company, Milwaukee, U.S.A.) and tetraethylortosilicate (TEOS, $(C_2H_5O)_4Si$, purity > 98 %, Merck-Schuchardt, Hohenbrunn, Germany) were used as starting materials. 2 wt. % polyvinyl alcohol (PVA, A.M.W. 70.000-100.000, Sigma Chemical Company, St.Louis, U.S.A.) solution in distilled water was used as the reaction medium.

PVA was dissolved in distilled water. 2 wt. % clear solution was obtained after stirring 20 minutes at 80 °C. 200 ml solution was used to produce 3 g $Y_3Al_5O_{12}$. $Y(NO_3)_3 \cdot 6H_2O$ and $Al(NO_3)_3 \cdot 9H_2O$ were added to the PVA solution according to the stoichiometry of YAG

($n_Y/n_{Al}=3/5$). $Ca(NO_3)_2 \cdot 4H_2O$ and TEOS were dissolved in solution to obtain required n_{Ca}/n_Y and n_{Si}/n_Y ionic ratios. We used equal moles of $Ca(NO_3)_2 \cdot 4H_2O$ and TEOS to determine co-solubility of Ca and Si in YAG.

Solutions were heated and stirred continuously until solution viscosity increased and yellowish jelly liquid was formed. Further heating on a hot plate resulted in a sponge like bulk solid whose color changed from yellow to brown. After this crispy solid was ground for 15 minutes, a very fine powder was obtained. Finally, these powders were calcined at 900 °C for 2 hours in a Pt crucible in air. After calcination process, white and fine YAG powders were obtained.

When the solubility limit is exceeded, phase separation is expected to occur due to the large distortion and the high vacancy concentration (if the host and the dopant ions have different valences) in the structure. The amounts of pre-existing phases are expected to decrease and new phases, which can allow higher amounts of the dopant in their structures, are formed. The co-solubility limit of Ca and Si in YAG was determined within 1 % accuracy using the disappearing-phase method [13].

X-ray diffraction analysis was carried out by a Bruker D8 diffractometer (XRD; Bruker AXS GmbH D8 Advance, Karlsruhe, Germany) employing Cu $K\alpha$ radiation ($\lambda=0.154056$ nm). The X-ray generator voltage and current were held at 40 kV and 40 mA, respectively. 2θ was varied continuously from 10° to 90° in locked-couple mode with a rate of 0.015 °/s. Diffrac plus evaluation software was used to analyze the diffraction data. Chemical composition of the powders were determined using an energy dispersive spectrometer (EDS; Roentech, QuanTax, Berlin, Germany) attached to a field emission scanning electron microscope (FEG-SEM; Leo Supra 35 VP, Oberkochen, Germany).

3 Results Two samples were prepared by doping the YAG with only Ca and only Si. Amounts of Ca and Si additions were well above the elemental solubilities of these elements. The compositions of the regions that have YAG stoichiometry were measured in these two samples by EDS. The results of these measurements were presented in Figs. 2(a) and (b). It was found out that Ca and Si concentrations in these regions were below the detection limit of EDS, which is consistent with the literature data (Table 1).

In order to find the co-solubility limit of calcium and silicon in YAG, Ca and Si amounts were varied between Ca (or Si)/Y = 2 % and Ca (or Si)/Y = 15 %. The EDS spectra of the 15 % co-doped sample can be seen in Fig. 2(c). It is obvious that more Ca and Si are present in the co-doped sample. The results of the quantitative EDS analyses are gathered in Table 1.

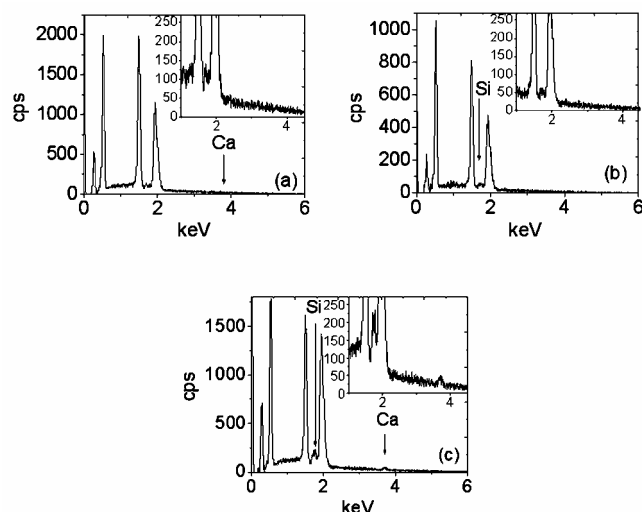


Figure 2 EDS spectra taken from (a) 10 % Ca doped sample (b) 7 % Si doped sample (c) 15 % (Ca+Si) co-doped sample.

The XRD spectra of co-doped samples are shown in Fig. 3. Only YAG phase is present up to 8 % Ca+Si addition. YAP peaks appeared in the diffraction pattern of the 9% co-doped sample. Intensities of YAP peaks decrease and YAM peak starts to appear when amounts of dopants exceed 9 %.

Table 1 Results of the quantitative EDS analyses for Ca doped, Si doped and Ca+Si co-doped samples. N.D.: Not detectable.

Element	Ca doped (at. %)	Si doped (at. %)	Ca+Si co-doped (at. %)
Y	39.83 ± 7.31	35.47 ± 2.10	37.38 ± 0.51
Al	60.17 ± 13.22	64.53 ± 7.32	56.88 ± 0.44
Ca	N.D.	N.D.	3.07 ± 0.33
Si	N.D.	N.D.	2.67 ± 0.42

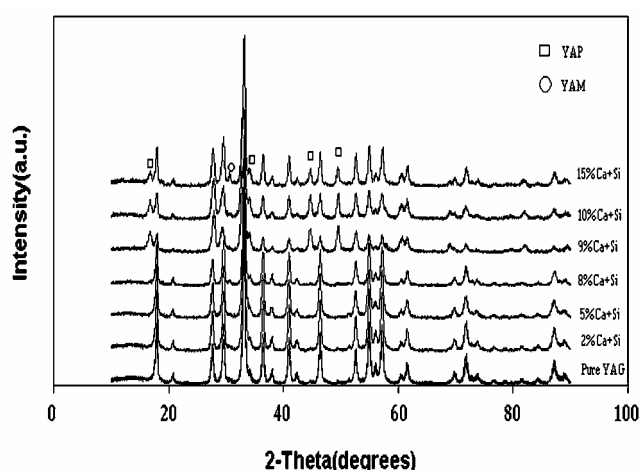


Figure 3 XRD spectra of co-doped samples with various dopant concentrations.

4 Discussion Ca has an ionic radius of 114.0 pm, when its coordination number is 6 [14]. It is approximately two times larger than Al ion. However, the ionic radius of Ca is very similar to that of Y, when their coordination numbers are 8. Therefore, it is more likely that Ca replaces Y. On the other hand, ionic radii of Si are 40.0 pm and 54.0 pm, ionic radii of Al are 53.0 pm and 67.5 pm, if their coordination numbers are 4 or 6, respectively [14]. Consequently, Si may substitute for Al.

Whenever there is a substitutional defect in the lattice, a strain is produced according to the difference between the ionic sizes of substituting elements. For instance, in the present case Ca has a larger ionic radius than Y. On the other hand, the ionic radius of Si is smaller than the host Al. Besides, charge neutrality should be maintained in the structure during a substitution. This condition is satisfied by the creation of some vacancies if substituting atoms have different charges. Formation of these vacancies has both a strain effect and a thermodynamic effect. Creation of a vacancy costs a definite amount of energy, which increases the Gibbs free energy of the lattice. On the other hand, this process increases the entropy of the system, which has a counter effect on the Gibbs free energy. Consequently, there is an equilibrium number of vacancies in the lattice which depends on the material and the temperature. When the vacancy concentration in the structure reaches a certain limit, the Gibbs free energy of vacancy formation is positive, and formation of one more vacancy is thermodynamically impossible [15]. As a result, no more substitution can be made, and phase separation occurs. These two limiting factors for the solubility are more critical if only Ca or only Si is added to the structure. However, vacancies are not created when both substitutions occur simultaneously because the charge of Ca is one less, and the charge of Si is one greater than those of the original cations; charge neutrality is already maintained. As a result, the vacancy limit of YAG is not an obstacle for dissolving Ca and Si when they enter to the structure at the same time. In the case of co-doping, size effect can also be diminished partially since Ca has a larger ionic radius than Y and the ionic radius of Si is smaller than the host Al. The increased co-solubility limit can be explained by the compensation of the size and charge mismatches accompanied to two substitutional defects. Ikesue *et al.* [16,17] and Wang *et al.* [18] have reported similar results for Nd and Si co-doped YAG. It should be noted that the size difference between Ca and Y ions is 8.7 % of the size of host Y ion while the size difference between Al and Si is 24.5 % of the size of host Al ion, when their coordination numbers are 4. EDS analysis of 15 % Ca+Si doped sample (Table 1) shows that YAG can accommodate approximately equal amounts of Ca and Si in its structure, which indicates that one Ca-Y replacement occurs for each Si-Al substitution. Consequently, Ca-Y replacement may not totally compensate for the size mismatch of Si-Al substitution, which may hinder the 100 % co-solubility of Ca and Si in YAG.

5 Conclusion Solubilities of Ca and Si are at least 8 times greater in YAG when they are added simultaneously. During simultaneous substitutions of Ca and Si charge neutrality is maintained and creation of vacancies is not necessary. In addition, when these two substitutions take place they can compensate for size mismatches of each other. These two effects can lead to the increased co-solubility limit. Ca-Y substitution can not fully compensate the size mismatch created by Si-Al replacement. Hence, % 100 co-solubility is not achieved.

References

- [1] T. I. Mah, T. A. Parthasarathy, and H. D. Lee, *J. Ceram. Process. Res.* **5**, 369 (2004).
- [2] X. Xu, Z. Zhao, P. Song, J. Xu, and P. Deng, *J. Alloys Compd.* **364**, 311 (2004).
- [3] J. K. R. Weber, B. Cho, A. D. Hixson, J. G. Abadie, P. C. Nordine, W. M. Kriven, B. R. Johnson, and D. Zhu, *J. Eur. Ceram. Soc.* **19**, 2543 (1999).
- [4] M. L. Keith and R. Roy, *J. Mineral. Soc. Am.* **39**, Nos. 1 and 2 (1954).
- [5] H. S. Yoder and M. L. Keith, *J. Mineral. Soc. Am.* **36**, Nos. 7 and 8 (1951).
- [6] J. Carda, M. A. Tena, G. Monros, V. Esteve, M. M. Reventos, and J. M. Amigo, *Cryst. Res. Technol.* **29**, 387 (1994).
- [7] G. L. Messing and H. Hausner (eds.), *Ceramic Processing Science and Technology* (American Ceramic Society, Westerville, 1995), p. 573.
- [8] L. Schuh, R. Metselaar, and G. de With, *J. Appl. Phys.* **66**, 2627 (1989).
- [9] S. R. Rotman, H. L. Tuller, and C. Warde, *J. Appl. Phys.* **71**, 1209 (1992).
- [10] K. R. Brown and D. A. Bonnell, *J. Am. Ceram. Soc.* **82**, 2423 (1999).
- [11] W. Y. Sun, X. T. Li, L. T. Ma, and T. S. Yen, *J. Solid State Chem.* **51**, 315 (1984).
- [12] Y. Wang, L. Zhang, Y. Fan, J. Luo, D. E. McCready, C. Wang, and L. An, *J. Am. Ceram. Soc.* **88**, 284 (2005).
- [13] B. D. Cullity, *Elements of X-Ray Diffraction* (Addison-Wesley, Reading, 1978), p. 377.
- [14] R. D. Shannon, *Acta Cryst.* **A32**, 751 (1976).
- [15] J.D. Verhoeven, *Fundamentals of Physical Metallurgy* (John Wiley & Sons, New York, 1975), p. 127.
- [16] A. Ikesue, K. Kamata, and K. Yoshida, *J. Am. Ceram. Soc.* **79**, 1921 (1996).
- [17] A. Ikesue, *Opt. Mater.* **19**, 183 (2002).
- [18] Y. Wang, L. Zhang, Y. Fan, J. Luo, P. Zhang, and L. An, *J. Am. Ceram. Soc.* **89**, 3570 (2006).